APPLICATION OF HIGH-ORDER COMPACT SCHEME TO INCOMPRESSIBLE TURBULENT FLOW

CHAO-HO SUNG* LI JIANG+ CHAOQUN LIU+

*David Taylor Model Basin, Carderock Division, NSWC, Bethesda, MD 20084

+ Department of Mathematics, University of Texas at Arlington, TX 76019

ABSTRACT

In this work, the high-order central compact scheme is introduced to improve the accuracy of the IFLOW solver. The high-order compact filter is used to reduce non-physical oscillations. To achieve the conservation property of the scheme, the compact scheme is combined with the ENO reconstruction method. The numerical flux at the cell interface is approximated by the derivative of its primitive function which can be exactly calculated. At the boundary, ghost points are constructed. The high-order extrapolation is used to obtain values at the ghost points. Instead of using the one-sided compact scheme, the explicit central difference scheme is applied at the boundary. The results from spatial simulations of trailing vortices have shown obvious improvement in accuracy.

1. INTRODUCTION

The compact schemes have been widely used in numerical simulation of complex flows. It has been shown [1] that the compact scheme can reach high-order accuracy and good small scale resolution with narrow grid stencils.

IFLOW code [2] is designed as a general-purpose production code for the numerical solutions of the incompressible Reynolds-averaged Navier-Stokes equations supplemented by appropriate turbulence models. The numerical methods include multi-block grid structure for complex geometry, artificial compressibility model, explicit one-step multi-stage Runge-Kutta scheme for time stepping, mutigrid, local time-stepping, implicit residual smoothing, optimal precondition, and bulk viscosity damping for convergence acceleration. The second order central difference and finite volume method are used for spatial discretization.

The fourth-order artifical dissipation terms are added to suppress numerical oscillations. The code has been used to analyze many complex flow fields including those around submarine, surface ship, and various parts of each.

In this work, the fourth-order compact finite difference scheme is incorporated into the code to improve the accuracy of the solutions. Instead of using artificial dissipation, the sixth order compact filter is used to reduce non-physical oscillations. To achieve the conservation property of the scheme, the compact scheme is combined with the ENO reconstruction method[3]. The numerical flux at the cell interface is approximated by the derivative of its primitive function which can be exactly calculated. The physical flux at the boundary is used as the boundary condition. To calculate the physical flux, ghost points are constructed by the fourth order extrapolation. The next section presents this method in detail, followed by the test cases and results of calculations.

2. GOVERNING EQUATIONS

The three-dimensional incompressible Reynolds-averaged Navier-Stokes equations based on the artificial compressibility approach can be expressed using the following conservative formulation.

$$P_0^{-1} q_t + F_x + G_y + H_z = 0 \tag{1}$$

where the preconditioned matrix P_0 and the three components of fluxes F, G, and H are defined as

$$P_0^{-1} = \begin{bmatrix} (1+\gamma)\beta^{-2} & \gamma\beta^{-2}u & \gamma\beta^{-2}v & \gamma\beta^{-2}w \\ (1+\alpha+\gamma)\beta^{-2} & 1+\gamma\beta^{-2}u^2 & \gamma\beta^{-2}uv & \gamma\beta^{-2}uw \\ (1+\alpha+\gamma)\beta^{-2} & \gamma\beta^{-2}vu & \gamma\beta^{-2}v^2 & \gamma\beta^{-2}vw \\ (1+\alpha+\gamma)\beta^{-2} & \gamma\beta^{-2}wu & \gamma\beta^{-2}wv & 1+\gamma\beta^{-2}w^2 \end{bmatrix}$$

$$q = \begin{bmatrix} p^* \\ u \\ v \\ w \end{bmatrix}, \quad F = \begin{bmatrix} u \\ u^2 + p^* - \tau_{xx} \\ uv - \tau_{xy} \\ uw - \tau_{xz} \end{bmatrix}, \quad G = \begin{bmatrix} v \\ uv - \tau_{yx} \\ v^2 + p^* - \tau_{yy} \\ vw - \tau_{yz} \end{bmatrix}, \quad H = \begin{bmatrix} w \\ uw - \tau_{zx} \\ wv - \tau_{zy} \\ w^2 + p^* - \tau_{zz} \end{bmatrix}$$

Here p^* is the pressure p divided by a constant density ρ. α, β^{-2} and γ are preconditioning parameters. In this presented work, $\alpha = \gamma = 0$ and

$\beta^{-2} = \max\left(|u|^2, \varepsilon\right)$, $\varepsilon = 0.7$. The Reynolds stresses calculated by turbulence model are given by τ_{ij}, $i, j = x, y, z$.

3. NUMERICAL METHOD

In the old version of IFLOW, a finite volume method is used. The mean flow is descretized by a second-order accurate central difference method with the fourth-order dissipation terms. The turbulent flow is discretized by one of the several upwind schemes. The time step is based on an explicit one-step multi-stage Runge-Kutta method to reach a steady-state solution. Several convergence acceleration techniques including multigrid, local time step, implicit residual smoothing, preconditioning, and bulk viscosity damping have been implemented.

In this work, the fourth-order compact finite difference scheme [1] and the ENO reconstruction method [3] are used to approximate the derivatives of fluxes. To illustrate how to use this method, we choose F_x, the derivative of flux in the x direction, as the example. When a conservative approximation to the spatial derivative is applied, F_x can be expressed as

$$F_x\big|_j = \frac{1}{\Delta x}\left(\hat{F}_{j+\frac{1}{2}} - \hat{F}_{j-\frac{1}{2}}\right) \tag{2}$$

where $\hat{F}_{j+\frac{1}{2}}$ and $\hat{F}_{j-\frac{1}{2}}$ are numerical flux functions at the cell interfaces. In order to achieve the high-order accuracy, numerical fluxes should be defined in such a way that the difference of numerical fluxes is a high-order approximation of the derivative F_x. According to the ENO reconstruction procedure [3], it has been proved that the primitive function of $\hat{F}$ at the cell interfaces can be exactly calculated by the value of F_j at given points. If P is the primitive function of $\hat{F}$, then:

$$\mathrm{P}_{j+\frac{1}{2}} = \Delta x \sum_{i=-\infty}^{j} \hat{F}_i \tag{3}$$

Then the numerical flux $\hat{F}$ at the cell interface can be obtained by taking derivative of its primitive function P,

$$\hat{F}_{j+\frac{1}{2}} = \mathrm{P}'_{j+\frac{1}{2}} \tag{4}$$

The approximations of derivatives of P at cell interfaces are calculated by the fourth-order compact finite difference scheme. G_y and H_z are discretized in the same manner. The sixth order compact filter is used to reduce numerical oscillations.

4.NUMERICAL EXAMPLES

To verify the efficiency of this high-order approach, the development of a trailing vortex is simulated using the k-ω turbulence model. In the first testing problem, a laminar q-vortex solution of Batchelor[2] is used as the inlet flow condition, i.e.

$$V_\theta = V_{\theta 1}(1+\frac{1}{2\alpha})\frac{r_1}{r}\left[1-\exp\left(-\alpha\frac{r^2}{r_1^2}\right)\right] \qquad U-U_\infty = U_D\left(-\alpha\frac{r^2}{d^2}\right)$$

where $r^2 = y^2 + z^2, \alpha = 1.25643, V_{\theta 1} = 0.286,$ $U_D = 0.165,$ and $r_1 = 0.036$. The size of the computational domain is $40\times1\times1$. The inlet is located at x=5. The grid number is $96\times32\times32$. Fig.1 and 2 show the distributions of the streamwise and tangential velocities along a vertical line through the vortex core at different locations in the x direction. The results from the second-order and the fourth-order are displayed in the same figure. Fig.3 shows the contours of vorticity at different x locations. The first row is corresponding to the second-order results, and the second row is of the fourth-order. It can be seen from these results that the high-order compact scheme increases the accuracy of the solutions and has demonstrated a better resolution than second-order scheme.

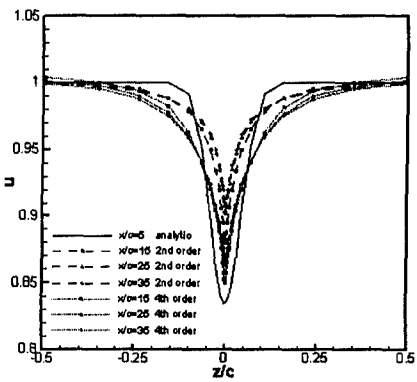

Fig.1 Streamwise velocity

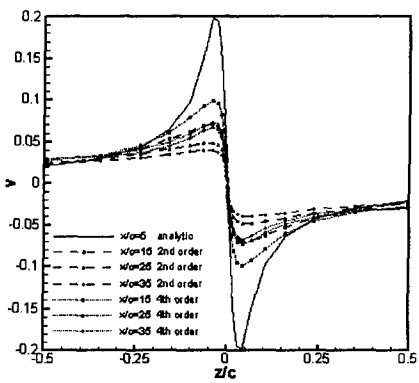

Fig.2 Tangential velocity

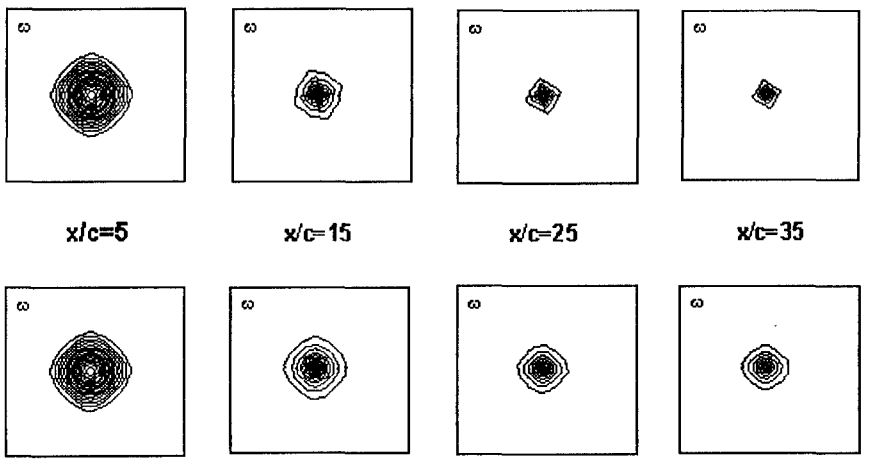

Fig.3 Contours of vorticity at different x locations

In the second testing problem, the experimental data from [2] are used to prescribe the inlet flow. The geometry and flow condition match those in the experiment. The computational domain extends from x/c=5 to x/c=45 in the streamwise direction. The grid is clustered near the center of the vortex on the cross section. In the streamwise direction the grid is uniform. The grid number is $56\times56\times56$. Experimental data (17×17) at x/c=5 are interpolated to the computational grid nodes. The numerical results are compared with experimental data at x/c=10. Fig.4 and 5 show the distributions of the streamwise and tangential velocities along a vertical line through the vortex core at different locations in the x direction. The results from the second-order and the fourth-order are compared with the experimental results. It is obvious that the accuracy is improved by using the high-order compact scheme. The large discrepancy between numerical results and experiment data is caused by errors of the interpolated inlet boundary condition, as we find this discrepancy also exists at the sections very close to the inlet boundary.

5.CONCLUSIONS

The fourth-order compact scheme in the conservative form has been incorporated in to the production code IFLOW. The results from the testing cases have shown the improvement in accuracy. The further applications of this method to more complex flows are undertaken.

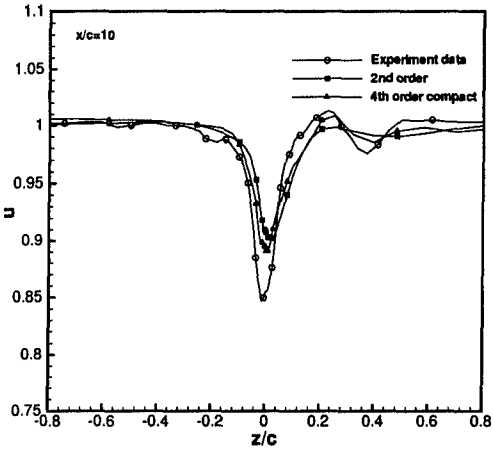

Fig.4 Streamwise velocity

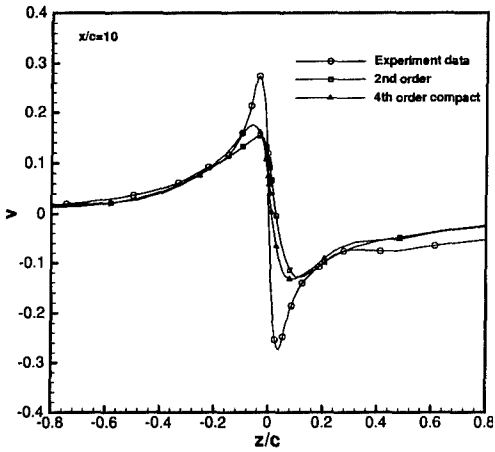

Fig.5 Tangential velocity

References

1. Lele, S.K., Compact finite difference schemes with spectral-like resolution. J.Comput. Phys., 103, pp.16-42, 1992
2. Sung, C.H., Rhee, Bong, Proceedings of the Seventh International Conference on Numerical Ship Hydrodynamics. Nantes, France, July 19-22, 1999.
3. Shu, C. W., Osher, S, Efficient implementation of essentially non-oscillatory shock capturing schemes II, I. Comput. Phys., 83, 32-78, 1989.
4. Devenport, W. J., et al, 1996, The structure and development of a wing-tip vortex. J. Fluid Mech.312,67-106.